Dynamic soil-structure interaction in offshore wind turbines on monopiles in layered seabed based on real data*

Guillermo M. Álamo[1], Juan J. Aznárez[1,*], Luis A. Padrón[1], Alejandro E. Martínez-Castro[2], Rafael Gallego[2], Orlando Maeso[1]

[1] Insituto Universitario de Sistemas Inteligentes y Aplicaciones Numéricas en Ingeniería (SIANI), Universidad de Las Palmas de Gran Canaria, Edificio Central del Parque Científico y Tecnológico, Campus Universitario de Tafira 35017 Las Palmas de Gran Canaria, Spain
guillermo.alamo / luis.padron / juanjose.aznarez / orlando.maeso @ulpgc.es

[2] Departamento de Mecánica de Estructuras e Ingeniería Hidráulica, ETS de Ingenieros de Caminos, Canales y Puertos, Universidad de Granada, Avenida Fuentenueva s/n, 18002 Granada, Spain
amcastro / gallego @ugr.es

Abstract

The present paper studies the soil-structure interaction (SSI) effects on the dynamic properties of offshore wind turbines (OWT) founded on monopiles. For that purpose, a three degrees-of-freedom substructuring model based on modal parameters is proposed. The whole superstructure is reduced to a punctual mass by its fundamental modal mass and height, while the pile-soil stiffness is represented by the corresponding impedance functions. The proposed model, together with characteristic relations between the fixed-base fundamental frequency and the modal parameters obtained from data of existent OWTs found in the literature, is used to analyse the influence of the superstructure and foundation dimensions and soil profile on the magnitude of the SSI phenomena. The obtained results confirm the relevance of including the foundation stiffness in the design stage of OWT systems, as variations in the fundamental frequency close to 15% can be produced. The homogeneous assumption, even if $c_{s,30}$ mean values are assumed, yields to misleading results if the actual soil profile presents properties that vary with depth. The superficial layers of the soil profile are found to play a major role in the estimation of the OWT system fundamental frequency and damping when the SSI phenomena are included.

Keywords: offshore wind turbines, soil-structure interaction, monopile impedance functions, modal analysis, multilayered half space

*Pre-print of the paper published in OCEAN ENGINEERING, 156, 14-24 (2018), DOI: 10.1016/j.oceaneng.2018.02.059

1 Introduction

In the last years, the use of Offshore Wind Turbines (OWT) has experienced a great increment owing to the reduction in cost and the increase in the generators size and power. However, further research is demanded in order to better understand the dynamic behaviour of their supporting structure and so that design and lifespan can be improved.

The principal foundation type for OWTs is the monopile (80.1% of the OWT installed in Europe are founded on monopiles according to EWEA [1]). Monopile foundations consist of a short hollow pile with large diameter that is driven into the seabed, and are commonly used for water depths of 20-40 meters. The simplicity of the construction and assembly is the principal advantage of this foundation type. However, the pile is a very slender structure and, consequently, more flexible than other foundation configurations (e.g. gravity based or jackets). The soil-structure interaction (SSI) effects have to be carefully considered when studying the dynamical behaviour of the OWT, being these effects highly dependent of the foundation typology used.

One of the principal effects of the SSI is the change of dynamic properties, i.e. fundamental frequency and damping, of the foundation-structure system with respect to the fixed-base structure. The variation in the eigenfrequency has to be carefully considered when designing the OWT structure in order to avoid resonance with the excitation frequencies and the corresponding increase in fatigue damage. Besides the wind and wave loads that present a frequency content below 0.1 Hz, the principal frequencies to avoid are the rotor frequency (1P) and the blade-passing frequency (3P or 2P depending on the number of blades). The first corresponds to rotor or aerodynamic unbalance loads, while the latter is produced by the shadowing effect from the wind of the blades passing the tower. The DNV [2] recommendation is to keep the tower frequency outside the $\pm 10\%$ range of these frequencies. Additionally, depending on the relation between the tower fundamental frequency and the aforementioned frequencies, three classical designs are distinguished [3, 4]: soft-soft if the tower frequency is below the 1P, soft-stiff if it is between 1P and 3P, and stiff-stiff when the structural eigenfrequency is higher than 3P. The soft-soft design is usually avoided as it corresponds to very flexible structures and shows the eigenfrequency near to the wind and wave loads. On the other hand, the stiff-stiff design is not a common choice owing to the high material requirements in order to reach the desired frequencies. Thus, the soft-stiff design is the one that is usually adopted. This design causes the OWT natural frequency to be within a very narrow range, highlighting the importance of an accurate estimation.

Despite giving a proper literature review is out of the scope of the present paper, the authors want to refer the interested readers to the works of Galvín et al. [5], Bisoi and Haldar [6], Damgaard et al. [7], or Zaaijer [8], where numerous recent studies addressing the influence of the SSI effects on the variation of the OWT tower eigenfrequency and damping are presented.

The present work proposes a simplified substructuring model based on modal parameters to analyse the variations in the fundamental frequency and damping of OWT systems due to the SSI effects. The whole superstructure is reduced to a punctual mass through its modal mass and height. On the other hand, the foundation stiffness is addressed through impedance functions obtained numerically by an integral time-harmonic model. This model makes use of Green's functions for the layered half space to represent the

soil behaviour and treats the pile, discretized by the FEM as a Timoshenko beam, as a load line acting within the soil. The one degree-of-freedom mass and the impedance functions are then coupled together into the proposed simplified substructuring model, and the modal approach is validated against a more elaborated substructuring FEM model considering the complete superstructure dimensions. Then, the proposed methodology is applied to study the influence of the soil-structure system properties on the magnitude of the SSI effects, paying special attention to the soil profile. The analyses are carried out by assuming characteristic structural properties obtained from data of actual OWT systems and soil profiles based on boreholes of the North Sea.

2 Problem Statement

2.1 Problem definition

This paper addresses the dynamic characterization of OWT structures founded on monopiles. The system is assumed to be composed by a conical hollow tower, rotor and generator nacelle located at the tower top, and a monopile acting as foundation (see Fig. 1). The tower is connected to the monopile through a transition piece, which is a cylindrical hollow beam presenting some working platforms that give access to the OWT structure for maintenance or repair activities. The monopile is assumed to be a cylindrical hollow beam that is driven into the seabed and that is composed by two different parts: the above-soil portion and the embedded portion, both presenting the same cross-section. The tower and pile are assumed to be made of the same material.

The system geometrical and material properties are: tower length H_t, tower top and bottom external diameters D_{top} and D_{bot}, ratio between the tower cross-section inner and outer diameters δ_t (henceforth, thickness ratio), mass of the blades and generator nacelle M_{RNA}, above-soil pile length H_p, pile embedded length L_p, pile external diameter D_p, pile thickness ratio δ_p, Young's modulus E and density ρ. Owing to the small aspect ratios that the embedded pile can present in this type of constructions, the Timoshenko's beam theory is used to model it. Thus, additional geometrical and material properties are required for the embedded pile: Poisson's ratio ν_p, shear coefficient α, and material hysteretic damping ratio ξ_p.

Finally, the problem is completely defined by knowing the water depth H_w and density ρ_w, and the soil profile given by the shear wave velocity c_s, which can change depending on the depth; and soil Poisson's ratio ν_s, soil density ρ_s and soil hysteretic damping ratio ξ_s, which are assumed to keep the same value for the whole profile.

The OWT system can be divided into two different parts: the superstructure (above soil) and foundation (under soil). By considering an infinite rigid base, the superstructure dynamic behaviour can be easily characterized by its fundamental frequency f_n and damping ratio ξ. However, if the foundation flexibility is included in the analysis, the SSI effects produce a reduction in the system fundamental frequency and changes in the damping ratio. The aims of this paper are computing these changes by obtaining the flexible-base fundamental frequency $\tilde{f}_n$ and equivalent damping ratio $\tilde{\xi}$, and studying how the superstructure, the foundation and the soil profile characteristics affect them.

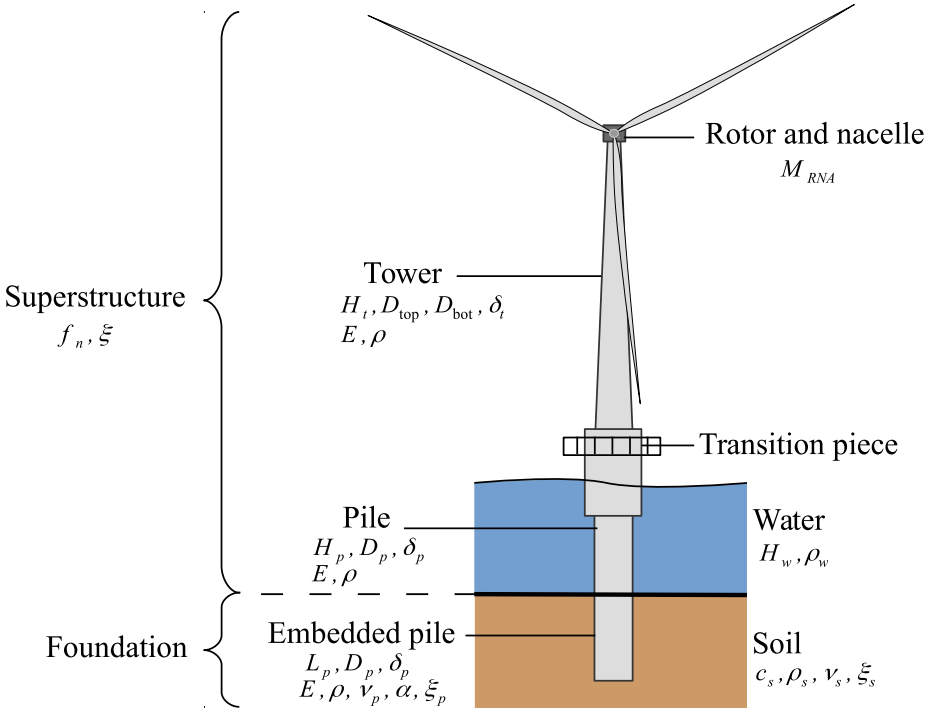

Figure 1: Representation of a generic OWT and identification of geometrical and material parameters.

2.2 Set of existent OWTs taken as starting point

Different OWT systems that can be found in the literature are selected for analysis in this study. Their properties and details are presented in Table 1. OWTs 1-12 were extracted from the work of Lombardi [9], and correspond to wind turbines from different wind farms already built in the UK. For each farm, a range of hub heights was indicated, so the maximum and minimum values are considered. Only information about diameters and thickness of the Vestas towers was available, so these dimensions are assumed for the Siemens towers too. On the other hand, OWTs 13 and 14 correspond to systems that have been widely studied in different works [e.g. 10–13]. Thus, more detailed information about them was accessible.

However, for the selected cases, there are very few details available about the dimensions of the transition piece and the length of the pile outside the seabed. For this reason, the transition from pile to tower is assumed to be produced at water level, so the pile length is equal to the water depth ($H_p = H_w$). On the other hand, some structures present a constant wall thickness, while others have a thickness that varies along the height. In order to define all the studied OWT systems in a coherent way, the thickness ratio is kept constant for the whole length. By doing so, thicker walls are presented at the tower base, where the largest diameter is located. The values of δ_t presented in Table 1 are obtained as the mean value of the ones corresponding to the tower top and bottom sections.

For all the structures, the towers and piles are assumed to be made of steel. Thus, a Young's modulus $E = 210$ GPa, a Poisson's ratio $\nu_p = 0.25$ and a density $\rho = 7850$ kg/m^3 are assumed. In addition, for the embedded piles, the hysteretic damping coefficient is

Table 1: Definition of the set of existent OWTs used in the present study.

OWT	1-2 Vestas 2MW-V66	3-4 Vestas 3MW-V90	5-6 Vestas 2MW-V80	7-8 Siemens SWT-3.6-107	9-10 Vestas 2MW-V80	11-12 Siemens SWT-3.6-107	13 North Hoyle 2MW-V80	14 Walney S 1 3.6MW
M_{RNA} (t)	80	111	94	220	94	220	100	234
H_t (m)	60-78	80-105	60-100	80-96	60-100	80-96	70	83.5
H_w (m)	11	10	20	19	21	25	11	20
L_p (m)	15	28	31	11	33	30	33	31
D_{top} (m)	2.3	2.3	2.3	2.3	2.3	2.3	2.3	3.0
D_{bot} (m)	4.2	4.2	4.2	4.2	4.2	4.2	4.0	5.0
δ_t (%)	98.0	98.0	98.0	98.0	98.0	98.0	97.6	97.9
D_p (m)	3.5	4.3	4.2	4.7	4.0	4.7	4.0	4.2
δ_p (%)	97.4	97.9	97.6	97.7	98.2	97.7	97.5	97.6

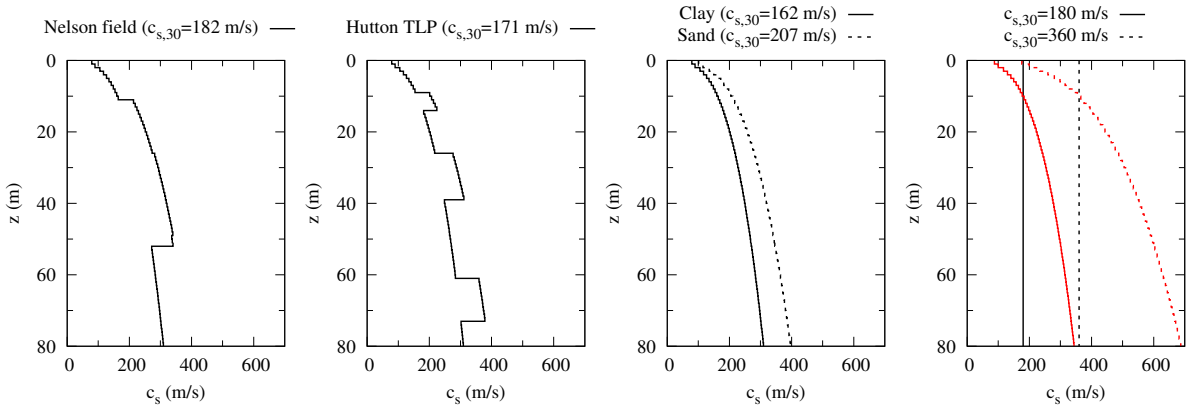

Figure 2: Soil profiles used in the study. Evolution of the shear wave velocity with depth.

set to $\xi_p = 2\%$ and the shear coefficient of a hollow circular cross-section $\alpha = 0.5$ is used. On the other hand, a fixed-base modal damping ratio of the structure $\xi = 1\%$ is assumed. For the water density, $\rho_w = 1000$ kg/m^3 is considered.

2.3 Soil profile definition

The soil profiles assumed for the sites in the analyses are presented in terms of the shear wave velocity c_s in Fig. 2. The value of the $c_{s,30}$ [14] for each profile is also displayed above each plot as it is widely used to characterize the soil. The selected profiles corresponds to C ($180 < c_{s,30} < 360$ m/s) or D soils ($c_{s,30} < 180$ m/s) which are the ones where OWT systems are usually founded on.

The principal profiles are two typical boreholes (Nelson Field and Hutton TLP) of the North Sea [see 15] which consist of different layers of clay and sand. The values of the shear wave velocity depend on the soil material and depth, and are estimated through Eq. (1), proposed by Ohta and Goto [16] and where $P = 1.000$, 1.260 or 1.286 for clay, fine sand and medium sand, respectively.

$$c_s = 78.98\ z^{0.312}\ P \qquad [\text{m/s}] \tag{1}$$

Additionally, two soils formed only by clay or medium sand are studied as limit scenarios. Finally, two homogeneous and two variable profiles with identical values of $c_{s,30} = 180$

and 360 m/s are selected in order to present results for a wider range of soils and being able to analyse the effects of the soil non-homogeneity. The latter variable profiles follow the evolution with depth presented in Eq. (1).

As depicted in Fig. 2, the studied profiles are discretized by piece-wise homogeneous layers of 1 m thickness (see Section 3.1). For depths greater than 80 m, the shear velocity is assumed to be constant with depth (half space domain). Soil density $\rho_s = 1800$ kg/m^3, Poisson's ratio $\nu_s = 0.35$ and hysteretic damping factor $\xi_s = 5\%$ are kept constant for the whole profile. These soil properties are similar to the ones used in other works for study monopiled OWT systems (see for instance Damgaard et al. [17, 18] or Zania [19]) and can be considered to be representative of common foundation grounds for this type of structures (modelled as equivalent elastic media) in regard to the aspects studied in this piece of research. The influence of the Poisson's ratio on the parameters analysed herein was studied and found to be negligible after obtaining virtually the same results for $\nu_s = 0.35 - 0.49$ (not shown for the sake of brevity), which agrees with the conclusions recently drawn by Damgaard et al. [18].

3 Methodology

The proposed methodology consists of a three-step procedure which results in a simplified model that allows to study the variation of the fundamental frequency and damping due to the foundation stiffness. Fig. 3 sketches out these steps: First of all, the fixed-base superstructure system is reduced to a single-degree-of-freedom system in terms of its shear effective modal mass and height (b). Then, the foundation stiffness is modelled through the corresponding impedance functions (c). Finally, both parts are coupled together into a three degrees-of-freedom substructuring model (d). In the following sections, each step is further detailed.

3.1 Foundation modelling

The foundation stiffness is represented by a set of impedance functions (K_{ij}) which relates the force (moment) in direction i with the displacement (rotation) in direction j. Impedance functions are frequency-dependent and complex-valued, with real and imaginary terms representing the stiffness and damping components, respectively. As the lateral response of the structure is studied, only the lateral, rocking and coupled lateral-rocking impedances are needed (Fig. 3c).

The impedance functions are obtained by a previously-developed three-dimensional time-harmonic numerical model [20] where the soil is represented by an integral formulation based on the dynamical reciprocal theorem and the use of Pak and Guzina [21] Green's functions for a multilayered half space. The pile is modelled by the FEM as a Timoshenko beam and considered as a load line within the soil domain, so that its presence does not alter the soil continuity. Linear behaviour of soil and piles is assumed as well as welded boundary contact condition in the pile-soil interface. Similar assumptions were made by Padrón et al. [22, 23].

The soil equations are obtained from the integral expression of the reciprocal theorem

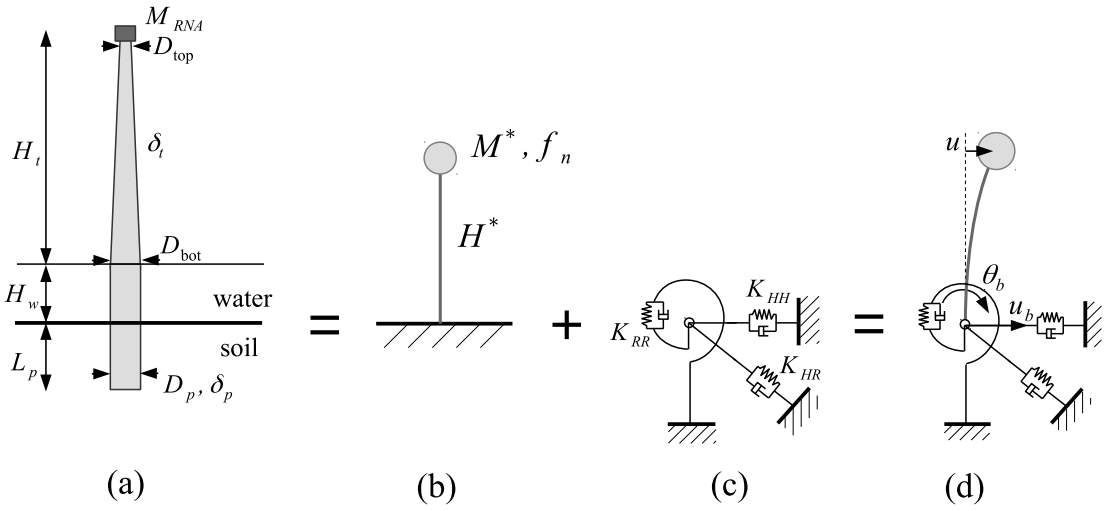

Figure 3: Stages of the proposed methodology. (a): System real geometry. (b): Superstructure representation through modal parameters. (c): Foundation stiffness representation through impedance functions. (d): Simplified substructuring model.

in elastodynamics [24]:

$$\int_{\Gamma} \mathbf{p}^* \mathbf{u} \, \mathrm{d}\Gamma + \int_{\Omega} \mathbf{b}^* \mathbf{u} \, \mathrm{d}\Omega = \int_{\Gamma} \mathbf{p} \mathbf{u}^* \, \mathrm{d}\Gamma + \int_{\Omega} \mathbf{b} \mathbf{u}^* \, \mathrm{d}\Omega \tag{2}$$

where $\mathbf{u}, \mathbf{u}^*$ are the displacements at any point of the domain under study Ω (layered half space); $\mathbf{p}, \mathbf{p}^*$ are the tractions acting over the boundary $\Gamma = \partial\Omega$; $\mathbf{b}, \mathbf{b}^*$ are the body forces acting inside the domain; and the star index $\square^*$ denotes the variables of the fundamental solution. Considering that the Green's functions used as fundamental solution already satisfy the free surface and layer interfaces boundary conditions; and that in the studied problem the only forces acting over the domain correspond to the load lines representing the piles, the expression of the reciprocal theorem can be reduced to:

$$\mathbf{u}^{\kappa} = \int_{\Gamma_l} \mathbf{u}^* \mathbf{q}_l^s \, d\Gamma_l \tag{3}$$

where $\mathbf{u}^{\kappa}$ are the displacements at the collocation point κ, $\mathbf{u}^*$ the tensor that contains the fundamental solution when the unit load is placed at point κ, and $\mathbf{q}_l^s$ the tractions along the load line Γ_l representing the pile-soil interaction tractions acting on the soil. Discretizing the pile and applying Eq. (3) to all the pile nodes results in the matrix equation:

$$\mathbf{u} = \mathbf{G}\mathbf{q}^s \tag{4}$$

being $\mathbf{u}$ the nodal displacements of the pile, $\mathbf{G}$ the matrix of coefficients obtained by integrating the fundamental solution times the elemental shape functions, and $\mathbf{q}^s$ the pile-soil tractions (acting on the soil) at the pile nodes.

On the other hand, the pile FEM equation is:

$$\bar{\boldsymbol{\mathcal{K}}}\mathbf{u} - \mathbf{Q}\mathbf{q}^p = \mathbf{F}^{\mathrm{top}} \tag{5}$$

where $\bar{\boldsymbol{\mathcal{K}}}$ is obtained from the stiffness and mass matrices as: $\bar{\boldsymbol{\mathcal{K}}} = \boldsymbol{\mathcal{K}}(1 + 2\mathrm{i}\xi_p) - \omega^2\boldsymbol{\mathcal{M}}$, being i the imaginary unit and ω the angular frequency; $\mathbf{Q}$ is the matrix that transforms the distributed soil-pile tractions acting along the pile $\mathbf{q}^p$ into nodal forces; and $\mathbf{F}^{\mathrm{top}}$ are the external forces acting on the pile head.

Both formulations are coupled imposing compatibility and equilibrium ($\mathbf{q}^s = -\mathbf{q}^p$) conditions along the load-lines, resulting in a system of linear equations. For the computation of each impedance term, the corresponding pile head displacements boundary conditions are established and the system of equations is solved for the pile head forces.

3.2 FEM model for the dynamic characterization of the superstructure

The application of the simplified three-step procedure mentioned above implies the need of defining effective masses and heights for every configuration. These are often obtained through explicit expressions derived for simplified geometries. In the present case, the realistic geometrical properties assumed herein for the problem under study do not allow following the same strategy. For this reason, the mass and height that will be used below for the characterization of the superstructure are obtained through a modal analysis based on a finite elements representation of the system, which will also allow the assumption of different properties for each structural section. At this step, fixed-base conditions will be assumed.

The superstructure, composed by the conical tower and the above-soil portion of the slender pile, is modelled as Bernoulli beams. For this type of structures, differences with respect to a more elaborated Timoshenko theory are negligible [11]. Constant-section two-noded four-degrees-of-freedom Hermitian beam elements are used for the discretization of both both the cylindrical (pile) and conical (tower) lengths. A high enough number of elements, set by proper convergence studies, is used to correctly represent the conical tower stiffness.

The generator and rotor masses are added as a punctual mass at the tower tip node. The hydrodynamic water added mass plus the mass of the internal water are also considered for the submerged elements. This additional mass is included by using a modified density $\bar{\rho} = \rho + \rho_w(C_m + \delta^2)/(1 - \delta^2)$ for the computation of the translational inertia mass matrix of the submerged beam elements. An added mass coefficient $C_m = 1$ is assumed in this study. The consideration of the additional water mass, despite significantly increasing the system total mass, does not affect the obtained results for the fundamental mode of vibration, as observed by Zania [19].

Considering harmonic displacement and forces, the fundamental frequency and its modal shape are obtained by solving the eigenvalues problem:

$$\left|\mathbf{K} - \omega^2\mathbf{M}\right| = 0 \tag{6}$$

where $\mathbf{K}$ and $\mathbf{M}$ are the superstructure stiffness and mass matrices obtained by the assembly of the elemental ones. As this equation is used to obtain the system modes of vibration, no damping is considered.

The fundamental frequency $\omega_n = 2\pi f_n$ and its modal shape $\boldsymbol{\phi}_n$ are obtained as the smallest eigenvalue (frequency) and its eigenvector (shape). Once the modal shape is

known, the base shear effective modal mass M^* and height H^* of the system to a base acceleration excitation can be obtained through [see, e.g. 25]:

$$M^* = \frac{\left(\boldsymbol{\phi}_n^T \mathbf{M} \boldsymbol{\iota}\right)^2}{\boldsymbol{\phi}_n^T \mathbf{M} \boldsymbol{\phi}_n}; \qquad H^* = \frac{\mathbf{h}^T \mathbf{M} \boldsymbol{\phi}_n}{\boldsymbol{\phi}_n^T \mathbf{M} \boldsymbol{\iota}} \tag{7}$$

where $\boldsymbol{\iota}$ is the influence vector presenting unitary values in the terms that corresponds to lateral displacements and zeros in the components corresponding to rotations; and $\mathbf{h}$ is the vector containing the height of each node in the terms that correspond to its lateral displacements and unitary values in the components corresponding to rotations.

The base shear effective modal mass (henceforth modal mass) coincides with the mass of a single-degree-of-freedom system that produces the same base shear force as the complete system vibrating at the corresponding modal frequency. On the other hand, the base-moment effective modal height (henceforth modal height) is the height of the aforementioned modal mass at which its inertia force produces the same base overturning moment as the distributed masses of the system at the modal frequency. The modal mass and height can also be obtained for all the modes of vibration by using expression (7) with the corresponding modal shapes. For higher modes negative modal heights can be obtained, which would imply that the base shear force and moment have opposite algebraic signs. The choice of these parameters to represent the system is made as the base shear force and moment are the reactions that interact with the foundation impedance functions.

3.3 Substructuring model for the analysis of the system

Once the modal parameters of the OWT in fixed-base conditions and the impedance functions representing the soil-foundation system are obtained, they are coupled together reducing the problem to a three degrees-of-freedom model representing the complete system as depicted in Fig. 3d, where u is the mass lateral displacement relative to the base and u_b and θ_b are the base displacement and rotation. In coherence with the model used for the computation of the fixed-base modal parameters, a given harmonic free-field ground lateral acceleration $\ddot{u}_g$ is defined as system excitation. The equations of motion of the simplified problem can then be expressed in matrix form as:

$$\left(\begin{bmatrix} K^* & 0 & 0 \\ 0 & K_{HH}(\omega) & K_{HR}(\omega) \\ 0 & K_{RH}(\omega) & K_{RR}(\omega) \end{bmatrix} - M^*\omega^2 \begin{bmatrix} 1 & 1 & H^* \\ 1 & 1 & H^* \\ H^* & H^* & (H^*)^2 \end{bmatrix} \right) \begin{Bmatrix} u \\ u_b \\ \theta_b \end{Bmatrix} = -M^* \ddot{u}_g \begin{Bmatrix} 1 \\ 1 \\ H^* \end{Bmatrix} \tag{8}$$

where $K^* = (2\pi f_n)^2 M^* (1 + 2\mathrm{i}\xi)$ is the lateral structural stiffness associated with the first mode that also includes the structural damping through the modal damping factor ξ, and $K_{HH}(\omega)$, $K_{RR}(\omega)$, $K_{HR}(\omega)$ and $K_{RH}(\omega)$ are the lateral, rocking and coupled dynamic stiffness and damping functions.

In order to obtain the flexible-base fundamental frequency and damping ratio, the methodology of finding an equivalent single-degree-of-freedom oscillator that reproduces the system response is used [see, e.g. 26, 27]. In this study, a hysteretically damped oscillator with natural frequency $\tilde{\omega}_n$ and damping ratio $\tilde{\xi}$ is assumed and the equivalence

Table 2: Validation of the proposed three-step formulation against the FEM model. Flexible-base fundamental frequency for the OWT systems. Results for the Nelson Field soil profile.

OWT	1	2	3	4	5	6	7	8	9	10	11	12	13	14
$\tilde{f}_n$ (Hz)	0.44	0.32	0.31	0.21	0.42	0.22	0.23	0.18	0.37	0.20	0.22	0.17	0.37	0.22
error (%)	0.38	0.25	0.12	0.07	0.53	0.16	0.19	0.12	0.34	0.12	0.16	0.09	0.24	0.19

is established in terms of the transfer function:

$$Q(\omega) = \left| \frac{\omega_n^2 u}{\ddot{u}_g} \right| = \left| \frac{1}{\left(1 - \dfrac{\omega^2}{\tilde{\omega}_n^2}\right) + 2\mathrm{i}\tilde{\xi}} \right| \tag{9}$$

which represents the shear force at the base of the structure per effective seismic force [25]. As the single-degree-of-freedom system can not reproduce the response of the substructuring model in all the frequency range, the maximum value Q_m of the transfer function is chosen as common point between both models. This maximum value is obtained by iteratively solving Eq. (8). The flexible-base fundamental frequency corresponds to the frequency at which this maximum value takes place, while the equivalent damping ratio is computed as $\tilde{\xi} = 1/(2Q_m)$.

In order to validate the ability of the proposed formulation to correctly capture the flexible-base fundamental frequency, an enhanced FEM model where the presence of the soil-pile system is included through the corresponding impedance functions is used. For that purpose, the displacement of the superstructure due to the ground horizontal acceleration and considering the foundation stiffness and damping is obtained by solving the equation:

$$\left(\mathbf{K}'(\omega) - \omega^2 \mathbf{M}\right) \mathbf{U} = -\mathbf{M}\boldsymbol{\iota}\ddot{u}_g \tag{10}$$

being $\mathbf{K}'(\omega)$ the superstructure stiffness matrix including the foundation dynamic stiffness and damping functions in the terms that correspond to the ground node and $\mathbf{U}$ the vector containing the nodal lateral displacements and rotations relative to the ground displacement. The flexible-base fundamental frequency is then obtained as the one at which the maximum response, in terms of $Q(\omega)$, takes place.

The flexible-base fundamental frequencies of the OWTs defined in Table 1 are computed through both the proposed three-step and the enhanced FEM formulations. Table 2 shows the computed modified eigenfrequencies together with the errors committed with respect to the enhanced FEM model, considering the Nelson Field soil profile. The results show negligible differences between both methodologies, revealing the ability of the proposed strategy to correctly represent the effects of the foundation on the system fundamental frequency. Results for harder soils were also obtained producing smaller differences, but are not presented for simplicity's sake.

It is important to notice that both the three-step and the FEM approaches are substructuring methodologies, as they incorporate the foundation impedance functions. The principal difference between them is that the three-step formulation makes use of the fundamental modal mass and height concepts (and therefore considers the fundamental mode only), while the FEM model does not, and takes all modes into account. The validation

results show that the flexible-base fundamental frequency can be accurately estimated by using the three-step approach owing to the fact that the first mode of the soil-structure system is principally influenced by the first mode of the fixed-base structure. However, the three-step methodology does not guarantee a correct estimation of the modified natural frequencies for higher modes. The principal advantage of the proposed three-step methodology lies in its efficiency and suitability for undertaking parametric studies.

4 Results

4.1 Analysis of the modal properties of the set of OWTs

The results of the modal analysis following the methodology presented in Section 3.2 for the studied OWT systems are shown in Table 3. For each structure, their fixed-base fundamental frequency and modal mass and height are listed. The latter parameters are also presented as the ratio with respect to the system total mass M_{total} (including the mass of submerged pile, tower, nacelle and water added mass), or the system total height H_{total} (obtained as the sum of the submerged pile and tower lengths). The fixed-base fundamental frequencies are found to be between 0.2-0.55 Hz, agreeing with the typical range for OWT constructions. On the other hand, the values of the modal mass and height are related to the structural dimensions. The modal mass is found to be 25-35% of the system total mass, while the modal height coincides with 85-90% of the system total height.

The obtained modal parameters for the studied OWT systems are plotted against each other in Fig. 4. A strong correlation is found for all the three possible combinations. A particularly high dependence between the modal height and fixed-base fundamental frequency is found. In order to derive an expression that relates the modal parameters, the computed modal mass and height values are fitted by first and second order polynomials as functions of the superstructure fixed-base eigenfrequency, yielding the following expressions:

$$H^*(f_n) = 130 - 138 f_n \qquad [\text{m}] \tag{11a}$$
$$M^*(f_n) = 4.24 - 4.84 f_n \qquad [10^5 \text{ kg}] \tag{11b}$$

$$H^*(f_n) = 161 - 341 f_n + 292 f_n^2 \qquad [\text{m}] \tag{12a}$$
$$M^*(f_n) = 5.92 - 8.97 f_n + 4.89 f_n^2 \qquad [10^5 \text{ kg}] \tag{12b}$$

Table 3: Modal parameters for the OWT systems.

OWT	1	2	3	4	5	6	7	8	9	10	11	12	13	14
f_n (Hz)	0.53	0.37	0.35	0.23	0.49	0.24	0.25	0.19	0.42	0.22	0.24	0.19	0.42	0.26
H^* (m)	60.8	75.4	80.1	100	66.3	100	91.0	105	65.2	98.7	94.3	109	70.8	89.1
H^*/H_{total}	0.86	0.85	0.89	0.88	0.83	0.84	0.92	0.92	0.81	0.82	0.90	0.90	0.87	0.86
M^* (t)	170	188	206	232	216	239	329	341	236	258	355	363	203	469
M^*/M_{total}	0.34	0.35	0.31	0.32	0.24	0.24	0.27	0.27	0.28	0.27	0.24	0.24	0.32	0.38

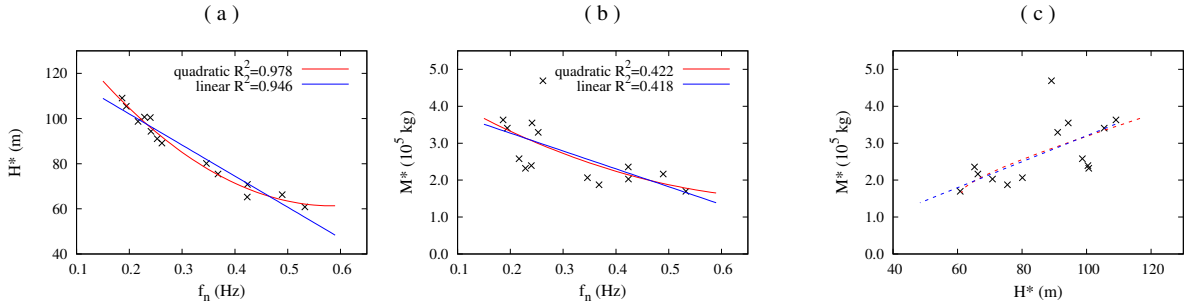

Figure 4: Modal parameters for the studied set of OWT (crosses). Polynomial regressions of the modal height (a, solid lines) or mass (b, solid lines) as a function of the fixed-base fundamental frequency. Relation between the modal mass and modal height obtained by using the regressed expressions (c, dashed lines).

The proposed polynomials are also plotted in Figs. 4a,b as solid lines, showing that modal height and mass can be fitted without significant errors by both the linear and quadratic expressions. Dispersion is higher for modal mass than for modal height. The modal mass corresponding to OWT number 14 is the only one that does not adequately fit in the obtained mass-frequency relations. This structure has a higher modal mass owing to its thick tower and pile walls when compared to the rest of the studied systems. Finally, Fig. 4c shows the relations between modal mass and height obtained by using the proposed polynomials. Eqs. (11) or (12) correctly represent the relation between both parameters. The use of these expressions is not recommended outside the frequency range 0.15-0.60 Hz shown in Figs 4a,b.

Now, and once the fixed-base fundamental frequency is set, modal mass and modal height can be accurately modelled through Eqs. (11) or (12), reducing the number of parameters needed to represent the superstructure. By doing so, instead of a discrete number of structures, a wider set of OWT systems representing the typical dimensions for this type of constructions can be included in the results presented in the following sections. Both the quadratic and linear expressions are used: the first fits the data better, while the constant slope of the latter allows to easily understand the contribution of each parameter.

4.2 Analysis of the pile dimensions of the set of OWTs

Now that the superstructure is completely defined, it is necessary to establish the dimensions of the monopile foundations. Following the same procedure as for the modal parameters, Fig. 5 presents the relation between the pile diameter (a) or pile embedded length (b) and the modal parameters for the OWT systems defined in Table 1. The data are fitted again by first and second order polynomials.

A high correlation is found between the pile diameter and the superstructure fixed-base fundamental frequency, showing that smaller pile diameters tend to correspond to shorter and more rigid structures. The fitting procedure yields to the following expressions, plotted as solid lines in Fig. 5a:

$$D_p(f_n) = 4.97 - 2.40 f_n \qquad \text{[m]} \tag{13}$$

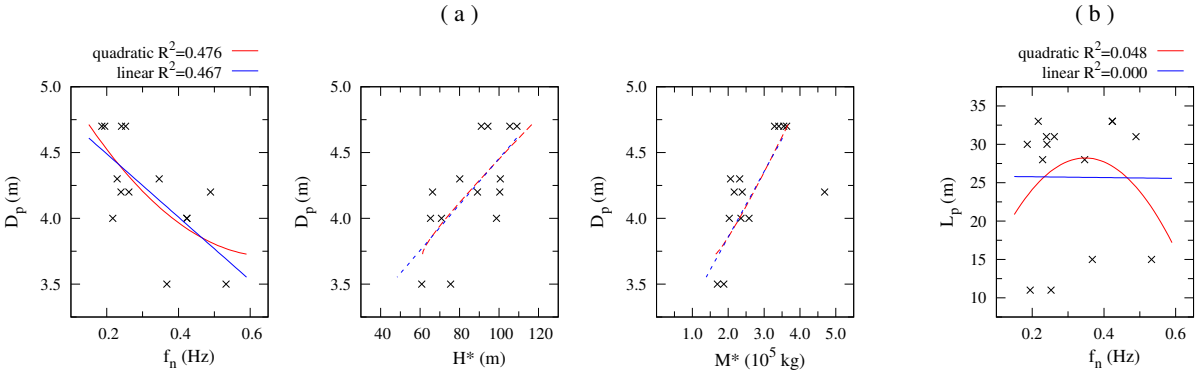

Figure 5: Pile diameter (a) and pile length (b) with respect to superstructure modal parameters for the studied OWT systems (crosses). Polynomial regressions of the pile diameter as a function of the fixed-base fundamental frequency (a, solid lines). Relations between the pile diameter and modal height or mass obtained by using the regressed expressions (a, dashed lines). Polynomial regressions of the pile embedded length as a functions of the fixed-base fundamental frequency (b, solid lines).

$$D_p(f_n) = 5.40 - 5.15 f_n + 3.93 f_n^2 \qquad [\text{m}] \tag{14}$$

The use of these expressions together with Eqs. (11) and (12) adequately represents the relations between the pile diameter and superstructure modal mass and height too, as shown by the dashed lines in Fig. 5a.

On the other hand, the pile length can not be correctly adjusted by the polynomial fitting as a function of the fixed-base fundamental frequency. In this type of constructions, the pile embedded length is more dependent on the soil properties than on the superstructural dimensions. Thus, different values of the pile length can be assumed independently of the fixed-base fundamental frequency.

Finally, the pile wall thickness value is established following the API [28] recommendation as a function of the pile diameter:

$$t_p \approx 6.37 + \frac{D_p}{100} \quad [\text{mm}] \tag{15}$$

Note that $\delta_p = (D_p - 2t_p)/D_p$.

4.3 Definition of the characteristic properties for the parametric analysis

As commented in the previous section, if Eqs. (11) or (12) are used, the superstructure can be defined by setting the fixed-base fundamental frequency and the structural modal damping. Values between 0.15-0.60 Hz are used as a common range within which the OWT fixed-base eigenfrequency is found. On the other hand, for the fixed-base modal damping ratio a value of $\xi = 1\%$ is chosen following the recommendation of the GL [29] Guideline.

The pile diameter and wall thickness are also known once the fixed-base fundamental frequency is set by using Eqs. (13) or (14) and (15), respectively. Aiming at studying

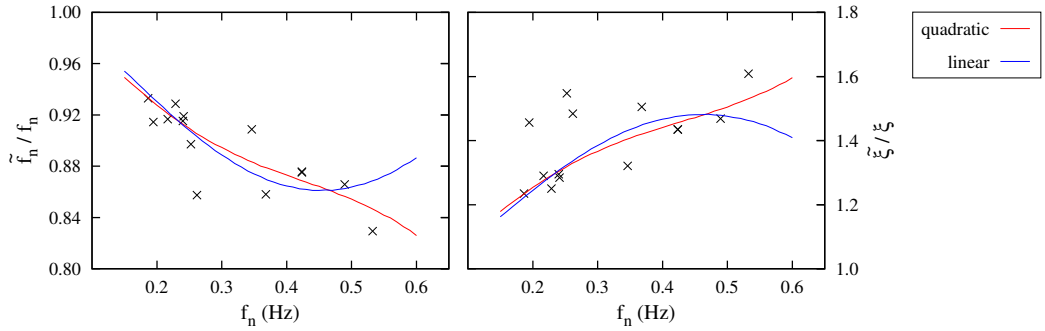

Figure 6: Flexible-to-fixed-base natural frequencies ratio and equivalent-to-structural dampings ratio. Comparison between the results of the regressed (lines) and real (crosses) modal parameters and pile dimensions. Results for the Nelson Field soil profile. Pile length $L_p = 25$ m for the regressed dimensions.

different foundation geometries, three values of pile embedded length $L_p = 15, 25$ and 35 m are considered.

4.4 Influence of the superstructures parameters on the magnitude of the SSI phenomena

In order to explore the influence of the OWT fundamental frequency and damping on the magnitude of the SSI phenomena, Fig. 6 presents the ratios $\tilde{f}_n/f_n$ (flexible-to-fixed-base natural frequencies ratio) and $\tilde{\xi}/\xi$ (equivalent-to-structural dampings ratio) as a function of the fixed-base fundamental frequency of the superstructure computed as detailed in Section 3.3. The results are obtained assuming the Nelson Field soil profile. The crosses correspond to the results for the studied OWT systems whose modal properties are defined in Table 3 and pile dimensions in Table 1. On the other hand, the lines present the results that are obtained by using the regressions (11) to (15) and assuming a pile embedded length $L_p = 25$ m. Attending to Fig. 6, the curves from the fitted polynomials follow the overall trends of the points representing the actual OWT systems, both in the frequency and damping variations. Thus, the use of the fitting expressions is justified for the general study of the SSI effects on the dynamic properties of OWT structures.

At low frequencies ($f_n < 0.45$ Hz), virtually the same results are obtained from the use of both the linear or quadratic fitting. However, at higher frequencies ($f_n > 0.45$ Hz), the curves diverge owing to the differences that are produced at these frequencies in the regression polynomials, specially the ones of the modal mass and height (see Fig. 4). The quadratic expressions are found to better adjust the real points, but, as only two points are available within this frequency range, one can not discern if it represents the real trend or if it is produced by overfitting issues.

In order to explain the curve shapes and the differences observed between the results of the real and fitted data, one has to consider the influence of each modal parameter (fixed-base frequency, modal mass and height) on the magnitude of the SSI phenomena. All of these parameters have the same effect: increasing its value amplifies the magnitude of the SSI (i.e. fundamental frequency reduction and damping gain). This can be

Table 4: Impedance functions at the flexible-base fundamental frequency of the studied OWT systems. Nelson Field soil profile. (Units in GN, m)

OWT	1	2	3	4	5	6	7	8	9	10	11	12	13	14
$\tilde{f}_n/f_n$	0.829	0.858	0.909	0.929	0.866	0.915	0.897	0.914	0.876	0.917	0.919	0.933	0.875	0.857
$\tilde{\xi}/\xi$	1.608	1.505	1.321	1.250	1.469	1.295	1.547	1.456	1.435	1.290	1.284	1.234	1.434	1.484
Re$[K_{HH}]$	0.862	0.866	1.193	1.196	1.149	1.156	1.286	1.287	1.075	1.080	1.361	1.363	1.075	1.156
Im$[K_{HH}]$	0.077	0.075	0.102	0.099	0.102	0.096	0.107	0.105	0.093	0.089	0.114	0.112	0.093	0.096
Re$[K_{RR}]$	32.01	32.03	59.96	59.99	55.69	55.75	73.32	73.34	48.17	48.21	78.45	78.47	48.17	55.75
Im$[K_{RR}]$	1.685	1.650	3.111	3.051	2.954	2.835	4.259	4.211	2.518	2.439	4.008	3.967	2.518	2.837
Re$[K_{HR}]$	-3.511	-3.520	-5.633	-5.642	-5.330	-5.349	-7.289	-7.295	-4.799	-4.812	-6.878	-6.883	-4.799	-5.349
Im$[K_{HR}]$	-0.241	-0.232	-0.376	-0.363	-0.371	-0.344	-0.470	-0.461	-0.325	-0.307	-0.447	-0.439	-0.325	-0.345

easily explained for the modal mass and fixed-base fundamental frequency: when one of these parameters augments while keeping the other constant, an increment of the system stiffness is produced. Thus, the foundation becomes relatively softer compared to the superstructure, resulting in more significant SSI phenomena taking place. On the other hand, the increasing importance of SSI effects for higher wind turbines is in line with the results of Zania [19], and also agrees with the conclusions of Veletsos and Meek [26] or Stewart et al. [30] showing that the SSI effects becomes more evident as the wave parameter ($\sigma = c_s/Hf_n$) decreases.

Attending to this, the shape of the curves in Fig. 6 can be explained considering that, in their first part ($f_n < 0.45$ Hz) the magnitude of the SSI phenomena increases with the fixed-base natural frequency; while in the second part ($f_n > 0.45$ Hz) the effect of the reduction in the modal mass and height (Fig. 4) overtakes the effect of the increment in the eigenfrequency if the linear expressions are used. On the other hand, if the quadratic relations are considered, only the frequency effect is present as the modal mass and height remain practically the same in the high frequency range, explaining why the magnitude of the SSI phenomena continues increasing with the fixed-base natural frequency. These results also prove the importance of including the SSI effects in the preliminary designs of OWT structures. For $f_n < 0.25$ Hz, the $\tilde{f}_n/f_n$ ratio is found to be around 0.92 (8% reduction) while for $f_n > 0.25$, this reduction can be greater than 15%, with one data point at $f_n \approx 0.25$ yielding a $\tilde{f}_n/f_n$ ratio much smaller than the one obtained from the fitted expressions, and with the effects of SSI growing with the fixed-base fundamental frequency of the superstructure.

The results in terms of the flexible-to-fixed-base fundamental frequencies ratio ($\tilde{f}_n/f_n$) and equivalent-to-structural dampings ratio ($\tilde{\xi}/\xi$) for the set of studied OWT systems are also presented in Table 4 together with the real and imaginary components of each impedance term evaluated at the flexible-base fundamental frequency. This information gives an insight into the magnitude of the stiffness and damping contribution of the foundation and how it changes depending on the monopile dimensions. On the other hand, the impedance functions, together with the $\tilde{f}_n/f_n$ and $\tilde{\xi}/\xi$ ratios, corresponding to the use of the regressed expressions and assuming the different soil profiles can be consulted as supplementary material in the online version of the manuscript.

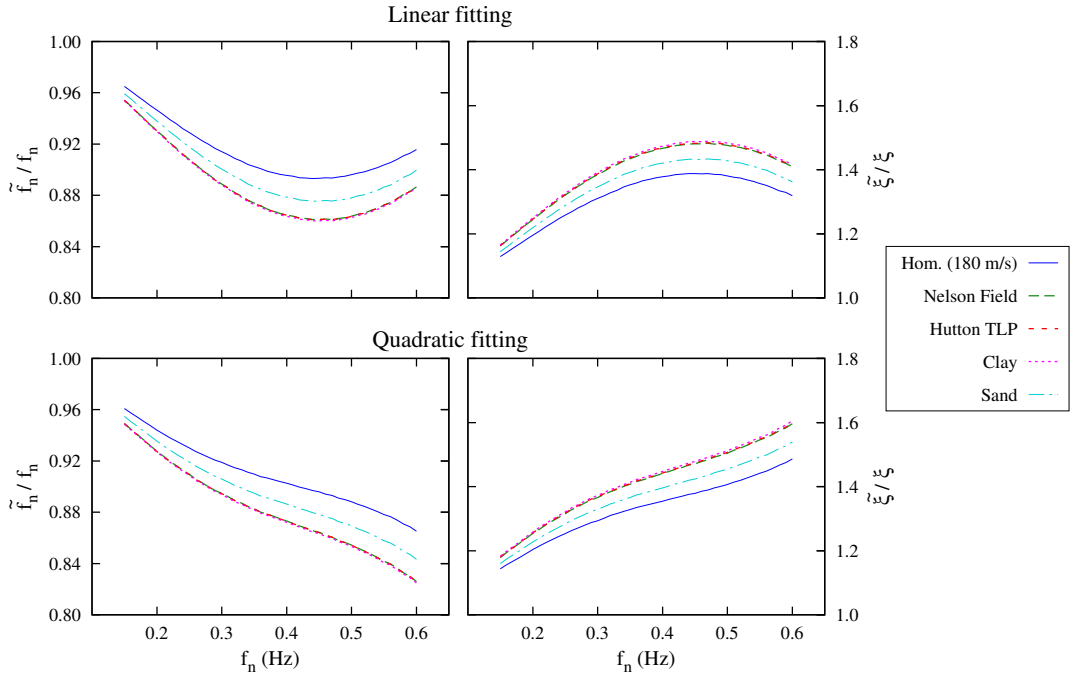

Figure 7: Influence of the soil profile on the flexible-to-fixed-base natural frequencies ratio and equivalent-to-structural dampings ratio. Pile length $L_p = 25$ m.

4.5 Parametric analysis of the influence of the SSI effects on the dynamic properties of OWT on monopiles

4.5.1 Influence of soil profile

Figs. 7 and 8 present the flexible-to-fixed-base natural frequencies ratio and the equivalent-to-structural dampings ratio as a function of the fixed-base fundamental frequency of the superstructure for the configurations described in Section 4.3. The results are grouped according to the use of the linear or the quadratic fitting. All soil profiles introduced in Section 2.3 are considered: first, Fig. 7 shows the results for the two typical North Sea's profiles (Nelson and Hutton), the Sand and Clay profiles, and the homogeneous soil with $c_{s,30} = 180$ m/s as its value is the closest to the one of the Nelson Field profile. Then, Fig. 8 compares the results obtained for the homogeneous and variable profiles with $c_{s,30} = 180$ and 360 m/s in order to study the effects of harder soils and the influence of the variable-with-depth profile.

The soil properties and profile evolution with depth have a direct influence on the magnitude of the SSI effects, producing higher variations as the soil becomes softer. However, the obtained results show the necessity of using a good measure to characterize the soil flexibility. Using the $c_{s,30}$ as a value to define the soil seems not to be a feasible option: profiles with close (e.g. Nelson Field and Homogeneous in Fig. 7) or even the same (Fig. 8) value of this mean shear wave velocity produce different frequency and damping variations depending on the evolution with depth of the profile. Moreover, the homogeneous assumption is a non-conservative hypothesis as those profiles produce smaller variations in both the fundamental frequency and equivalent damping than variable profiles with

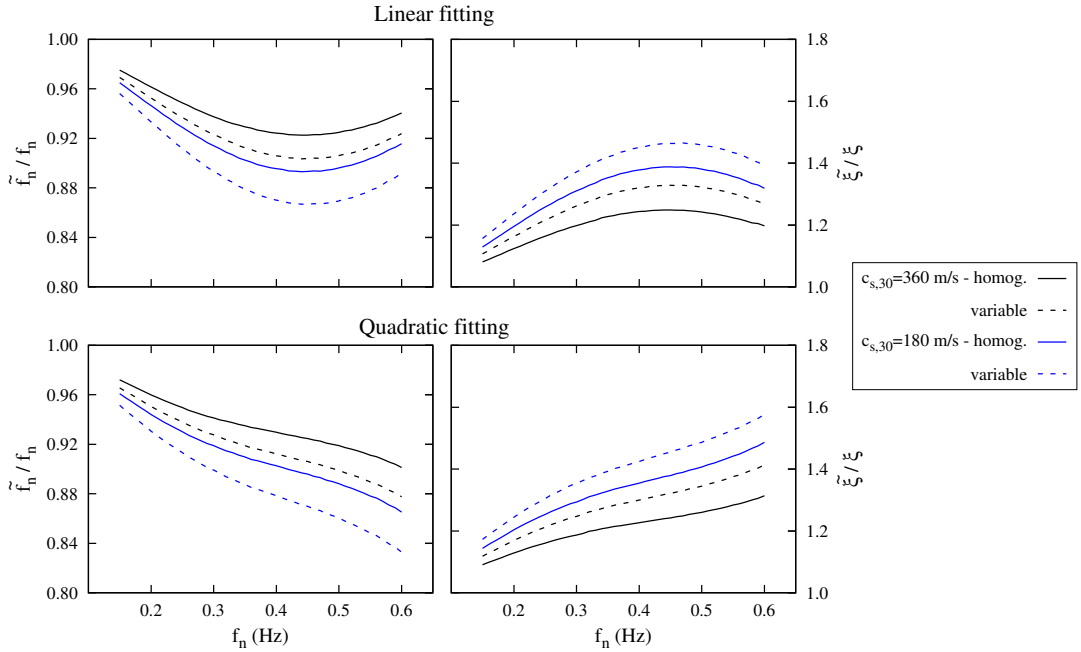

Figure 8: Influence of the soil profile on the flexible-to-fixed-base natural frequencies ratio and equivalent-to-structural dampings ratio. Comparison between soft and hard soils and between homogeneous (solid) and variable-with-depth (dashed) profiles with identical $c_{s,30}$. Pile length $L_p = 25$ m.

similar or higher values of $c_{s,30}$.

The superficial layers are the ones that govern the effects of the SSI on the dynamic properties of the studied structures. Fig. 7 shows that Nelson Field, Hutton TLP and clay profiles (which present identical properties along the first $\sim$ 10 meters) produce virtually the same variations in the system fundamental frequency and damping. This is related to the fact that the horizontal impedance of piles in non-homogeneous soils is principally determined by the superficial layers [31, 32], being this impedance term of crucial importance to the studied problem.

As expected, the magnitude of the SSI phenomena is less significant in harder soils (Fig. 8). However, variations over 10% in the system fundamental frequency and over 30% in the structural damping can be produced even for these hard soils. Fig. 8 shows again the importance of accurately knowing the actual soil profile. Results for the variable-with-depth soil with $c_{s,30} = 360$ m/s are closer to the ones for the $c_{s,30} = 180$ m/s homogeneous profile rather than to the homogeneous soil with the same mean velocity.

4.5.2 Influence of pile diameter

The pile diameter has a decisive role in the variations in the fundamental frequency and damping of the superstructure produced due to SSI effects. As the foundation stiffness strongly depends on the pile diameter, increasing its value results in a great reduction of the shifts in both the system eigenfrequency and damping. However, this role is not clearly seen in the previous results, as the diameter is implicitly defined as a function of

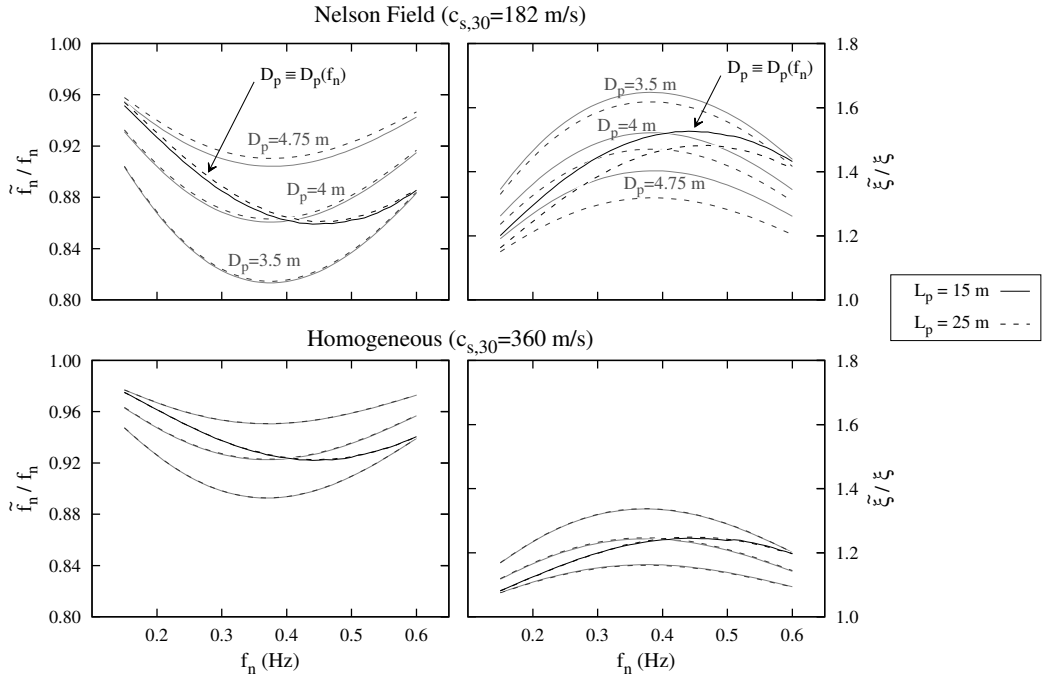

Figure 9: Influence of pile diameter and pile length on the flexible-to-fixed-base natural frequencies ratio and equivalent-to-structural dampings ratio. Linear fitting. $L_p = 15$ m (solid lines) and $L_p = 25$ m (dashed lines).

the fixed-base fundamental frequency. Fig. 9 presents the flexible-to-fixed-base natural frequencies ratio and the equivalent-to-structural dampings ratio obtained by assuming three frequency-independent pile diameters in addition to the results corresponding to the use of the diameter linear regression (Eq. 13). As the same effects are found for all the studied cases, only the results corresponding to the linear expressions and for two soils profiles: Nelson Field and Homogeneous ($c_{s,30} = 360$ m/s) representing soft and hard soils, respectively, are shown.

The curves obtained through the regressed pile diameter present an increment in the magnitude of the SSI phenomena as the fixed-base frequency augments, due to the reduction in the pile diameter (see Fig. 5). The effect of the pile diameter is almost independent of the pile length or the soil profile. However, for the softest soil profile, the differences between the results of the higher and lower diameters increase: e.g., for Nelson Field, the highest variation in the system fundamental frequency goes from 0.81 to 0.91 depending on the diameter, while for the Homogeneous ($c_{s,30} = 360$ m/s) this variation goes from 0.89 to 0.95.

4.5.3 Influence of pile length

Fig. 9 also presents the results obtained assuming two different pile embedment lengths: $L_p = 15$ m and $L_p = 25$ m.

Contrary to the diameter, the pile length has little importance on the effects of the foundation on the system fundamental frequency. Only for the highest diameter and softest soil profile, some differences can be seen between the 15 m piles and the longer

one. This is produced because of the fact that for higher diameters (smaller L/D ratios) the active length of the pile increases. Moreover, the differences between the 15 and 25 m lengths increase for the variable-with-depth profiles, where longer piles can reach stiffer layers. The above-mentioned effects are also manifested for the damping variations in a greater extent. $L_p = 25$ m is found to be larger than the active pile length in all cases, as results obtained for $L_p = 35$ m are completely coincident with those of $L_p = 25$ m (not shown for the sake of clarity).

On the other hand, for harder soils (Homogeneous $c_{s,30} = 360$ m/s), the active length for all diameters is below the 15 meters. Thus, no differences are observed between the studied lengths in both the frequency and damping variations.

5 Conclusions

In this paper a substructuring procedure based on modal parameters is presented and used to compute the variations in the structural fundamental frequency and damping due to SSI effects. The superstructure is represented by its fixed-base fundamental frequency and the first-mode base shear effective modal mass and height, while the foundation stiffness is considered through impedance functions. The proposed modal procedure is applied to OWT structures founded on monopiles and validated against an enhanced substructuring FEM formulation resulting in a good agreement.

Data from different medium-sized existent OWT systems that are found in the literature is used to obtain characteristic relations between the fixed-base fundamental frequency and the first mode effective height and mass. These relations are then employed to study the dynamic behaviour of general OWT structures founded on different monopiles and soil profiles. The obtained results confirm the importance of considering the foundation stiffness in the design stage of OWT systems in order to keep its fundamental frequency within the allowed range and to estimate the equivalent damping ratio of the structure. This is specially relevant for foundations consisting of small diameter monopiles on soft soils.

The magnitude of the SSI phenomenon is significant for $f_n > 0.25$ Hz, and specially for $f_n \approx 0.45$ Hz. This frequency range usually corresponds to a soft-stiff design, so special attention is required for those systems whose fundamental frequency is close to the 1P frequency. The recommendation of keeping the structural fundamental frequency $\pm 10\%$ away from the 1P and 3P (or 2P for two-bladed rotors) frequencies may not be enough if the foundation-structure fundamental frequency is not adequately computed, as the SSI effects can reduce the fixed-base fundamental frequency more than a 15%.

The present study also highlights the importance of an accurate knowledge of the soil properties and their evolution with depth when evaluating the foundation effects. Mean values, such as $c_{s,30}$, are insufficient for characterizing the soil stiffness. When the assumption of soil homogeneity is unavoidable, authors recommend the use of soil properties close to the ones corresponding to the superficial layers, as they are the ones that govern the changes in the fundamental frequency and damping ratio due to SSI effects.

Acknowledgements

This work was supported by the Ministerio de Economía, Industria y Competitividad (MINECO) and the Agencia Estatal de Invectigación (AEI) of Spain and FEDER through research projects BIA2014-57640-R and BIA2017-88770-R. G.M. Álamo is a recipient of the FPU research fellowship FPU14/06115 from the Ministerio de Educación, Cultura y Deporte of Spain. The authors are grateful for this support. Additional acknowledgement is given to Esteban García, former Master student at University Institute SIANI for his data compilation.

References

[1] EWEA, . The European offshore wind industry - key trends and statistics 2015. Report. European Wind Energy Association; 2016.

[2] DNV, . Guidelines for design of Wind Turbines. 2nd ed. Det Norske Veritas, Copenhagen and Wind Energy Department, Risø National Laboratory; 2002.

[3] Kühn, M.. Dynamics and design optimisation of offshore wind energy conversion systems. Ph. D. Thesis; Technical University of Delft; 2001.

[4] van der Tempel, J.. Design of support structures for offshore wind turbines. Ph. D. Thesis; Technical University of Delft; 2006.

[5] Galvín, P., Romero, A., Solís, M., Domínguez, J.. Dynamic characterisation of wind turbine towers account for a monopile foundation and different soil conditions. Struct and Infrastruct Eng 2017;13(7):942–954. doi:10.1080/15732479.2016.1227342.

[6] Bisoi, S., Haldar, S.. Design of monopile supported offshore wind turbine in clay considering dynamic soil-structure-interaction. Soil Dyn Earthq Eng 2015;73:103–117. doi:10.1016/j.soildyn.2015.02.017.

[7] Damgaard, M., Bayat, M., Andersen, L.V., Ibsen, L.B.. Assessment of the dynamic behaviour of saturated soil subjected to cyclic loading from offshore monopile wind turbine foundations. Comput Geotech 2014;61:116–126. doi:10.1016/j.compgeo.2014.05.008.

[8] Zaaijer, M.B.. Foundation modelling to assess dynamic behaviour of offshore wind turbines. Appl Ocean Res 2006;28(1):45–57. doi:10.1016/j.apor.2006.03.004.

[9] Lombardi, D.. Dynamics of Offshore Wind Turbines. MSc Thesis; University of Bristol; 2010.

[10] Adhikari, S., Bhattacharya, S.. Dynamic analysis of wind turbine towers on flexible foundations. Shock Vib 2012;19(1):37–56. doi:10.3233/SAV-2012-0615.

[11] Arany, L., Bhattacharya, S., Adhikari, S., Hogan, S.J., Macdonald, J.H.G.. An analytical model to predict the natural frequency of offshore wind turbines on three-spring flexible foundations using two different beam models. Soil Dyn Earthq Eng 2015;74:40–45. doi:10.1016/j.soildyn.2015.03.007.

[12] Bisoi, S., Haldar, S.. Dynamic analysis of offshore wind turbine in clay considering soil-monopile-tower interaction. Soil Dyn Earthq Eng 2014;63:19–35. doi:10.1016/j.soildyn.2014.03.006.

[13] Lombardi, D., Bhattacharya, S., Wood, D.M.. Dynamic soil-structure interaction of monopile supported wind turbines in cohesive soil. Soil Dyn Earthq Eng 2013;49:165–180. doi:10.1016/j.soildyn.2013.01.015.

[14] Eurocode, . Eurocode 8: Design of structures for earthquake resistance. Part 5: Foundations, Retaining Structures and Geotechnical Aspects. Brussels: European Committee for Standardization; 2004.

[15] HSE, , Bond, A.J., Hight, D.W., Jardine, R.J.. Design of Piles in Sand in the UK Sector of the North Sea - Report OTH 94 457. Health and Safety Executive, London (UK); 1997.

[16] Ohta, Y., Goto, N.. Empirical shear wave velocity equations in terms of characteristic soil indexes. Earthq Eng Struct Dyn 1978;6(2):167–187. doi:10.1002/eqe.4290060205.

[17] Damgaard, M., Zania, V., Andersen, L.V., Ibsen, L.B.. Effects of soil-structure interaction on real time dynamic response of offshore wind turbines on monopiles. Eng Struct 2014;75:388–401. doi:10.1016/j.engstruct.2014.06.006.

[18] Damgaard, M., Andersen, L.V., Ibsen, L.B.. Dynamic response sensitivity of an offshore wind turbine for varying subsoil conditions. Ocean Eng 2015;101:227–234. doi:10.1016/j.oceaneng.2015.04.039.

[19] Zania, V.. Natural vibration frequency and damping of slender structures founded on monopiles. Soil Dyn Earthq Eng 2014;59:8–20. doi:10.1016/j.soildyn.2014.01.007.

[20] Álamo, G.M., Martínez-Castro, A.E., Padrón, L.A., Aznárez, J.J., Gallego, R., Maeso, O.. Efficient numerical model for the computation of impedance functions of inclined pile groups in layered soils. Eng Struct 2016;126:379–390. doi:10.1016/j.engstruct.2016.07.047.

[21] Pak, R.Y.S., Guzina, B.B.. Three-dimensional Green's functions for a multi-layered half-space in displacement potentials. J Eng Mech 2002;128(4):449–461. doi:10.1061/(ASCE)0733-9399(2002)128:4(449).

[22] Padrón, L.A., Aznárez, J.J., Maeso, O.. BEM-FEM coupling model for the dynamic analysis of piles and pile groups. Eng Anal Bound Elem 2007;31(6):473–484. doi:10.1016/j.enganabound.2006.11.001.

[23] Padrón, L.A., Aznárez, J.J., Maeso, O.. 3-D Boundary element-finite element method for the dynamic analysis of piled buildings. Eng Anal Bound Elem 2011;35(3):465–477. doi:10.1016/j.enganabound.2010.09.006.

[24] Wheeler, L.T., Sternberg, E.. Some theorems in classical elastodynamics. Arch Ration Mech Anal 1968;31(1):51–90.

[25] Chopra, A.K.. Dynamic of structures. Theory and applications to earthquake engineering. NJ: Prentice-Hall; 2001.

[26] Veletsos, A.S., Meek, J.W.. Dynamic behaviour of building-foundation systems. Earthq Eng Struct Dyn 1974;3(2):121–138. doi:10.1002/eqe.4290030203.

[27] Medina, C., Aznárez, J.J., Padrón, L.A., Maeso, O.. Effects of soil-structure interaction on the dynamic properties and seismic response of piled structures. Soil Dyn Earthq Eng 2013;53:160–175. doi:10.1016/j.soildyn.2013.07.004.

[28] API, . Recommended Practice for Planning, Designing, and Constructing Fixed Offshore Platforms - Working Stress Design, Ver. 21. USA: American Petroleum Institute; 2000.

[29] GL, . Guideline for the Certification of Offshore Wind Turbines. Germany: Germanischer Lloyd WindEnergie GmbH; 2005.

[30] Stewart, J.P., Seed, R.B., Fenves, G.L.. Seismic soil-structure interaction in buildings. II: Empirical findings. J Geotech and Geoenviron Eng 1999;125(1):38–48. doi:10.1061/(ASCE)1090-0241(1999)125:1(38).

[31] Kaynia, A.M., Kausel, E.. Dynamics of piles and pile groups in layered soil media. Soil Dyn Earthq Eng 1991;10(8):386–401. doi:10.1016/0267-7261(91)90053-3.

[32] Miura, K., Kaynia, A.M., Masuda, K., Kitamura, E., Seto, Y.. Dynamic behaviour of pile foundations in homogeneous and non-homogeneous media. Earthq Eng Struct Dyn 1994;23(2):183–192. doi:10.1002/eqe.4290230206.